

# Analytical investigation of damaged tunnel linings by the action of excessive earth pressure

H.Mashimo

*Public Works Research Institute, Tsukuba, Japan*

**ABSTRACT:** The objective of this paper is to clarify the mechanism of the failure of tunnel concrete lining by the action of excessive earth pressure and establish the method to estimate the direction and magnitude of earth pressure acting on tunnel concrete lining. In this study, field inspection was carried out at two existing road tunnels, which have suffered serious damages on concrete lining, and numerical analysis using two-dimensional FEM, which can take account of development of cracks, was carried out. The results showed that failure patterns of concrete lining obtained from numerical analysis gave the good agreement with those of actual tunnels and the direction and magnitude of earth pressure assumed to act on the damaged concrete lining were obtained.

## 1 INTRODUCTION

In Japan, there are some existing road tunnels in service that have suffered serious damage such as compression or shear failure on their concrete lining by the action of excessive earth pressure. For these damaged tunnels, some kind of countermeasures such as rock-bolting, inner lining, backfill grouting etc. were adopted to rehabilitate the damaged concrete lining. In order to adopt appropriate countermeasures against the damaged tunnel, it is important to clarify the cause of failure and evaluate the direction and magnitude of the load acting on the concrete lining. However, the mechanism of the failure of concrete lining by the action of excessive earth pressure has not been clarified yet and establishment of the method to evaluate the load acting on the concrete lining is necessary to select the countermeasure most suitable for the condition of damaged tunnel.

In the first part of this paper, field inspection on two existing damaged road tunnels was carried out and an overview of damaged tunnel concrete lining with compression failure at crown or shear failure at invert concrete lining was provided.

In the second, in order to clarify the mechanism of the failure of these damaged tunnels and estimate the direction and magnitude of earth pressure acting on the damaged concrete lining, numerical analysis using two-dimensional FEM, which can take account of development of cracks, was carried out. Furthermore, numerical analysis results were compared with the field inspection results and the mechanism

of the failure of concrete lining by the action of excessive earth pressure was discussed.

## 2 OUTLINE OF DAMAGED TUNNELS

In order to investigate the state of the deformation of existing tunnels, field inspection on the concrete lining surface was carried out at Tunnel A and Tunnel B.

### 2.1 *Description and inspection of Tunnel A*

Figure 1 shows the state of the deformation occurred in tunnel lining and geotechnical profile of Tunnel A. Tunnel A with a total length of 2,376m was constructed by steel and logging method about 30 years ago. Tunnel A has a horseshoe shape with a width of 9.7m and a height of 8.0m. Its support structure consists of concrete lining with a thickness of 60 cm.

In Tunnel A, passing-through tensile cracks at the shoulders and compressive failure at the crown due to bending moment were observed at the section with a distance of 800m from portal. The sling that suspended the ceiling boards showed buckling phenomena due to the upheaval of ceiling board. There was void between the ground and concrete lining around the crown. Figure 2 shows the detail of the compressive failure occurred at the crown. The ground at tunnel site and its vicinity, where the tunnel deformation occurred, appeared to be composed of mudstone with the uniaxial compressive strength of approximately 40N/mm<sup>2</sup>. The overburden height at the section where deformation occurred is 320m.

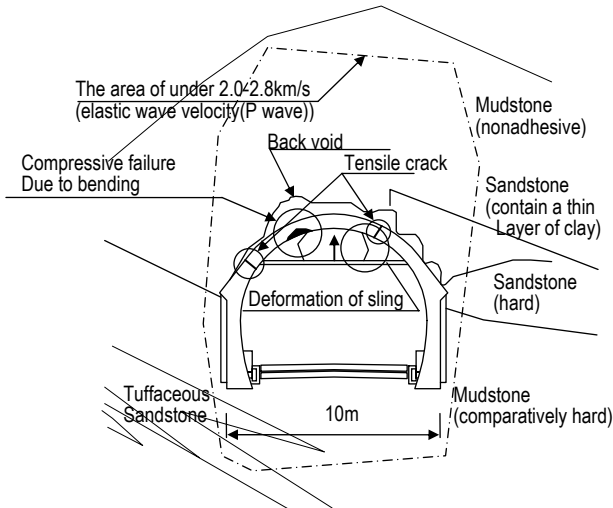


Figure 1. Deformation and geotechnical profile of Tunnel A.



Figure 2. Detail of failure occurred at tunnel crown in Tunnel A.

## 2.2 Description and inspection of Tunnel B

Figure 3 shows the state of the deformation occurred in tunnel lining and geotechnical profile of tunnel B. Tunnel B with a total length of 1,013m was constructed by steel and logging method about 15 years ago. Tunnel B has a horseshoe shape with a width of 11.3m and a height of 8.9m, and its support structure consists of concrete lining with a thickness of 60cm.

In Tunnel B, an upheaval of road surface was observed at the middle of the tunnel after about 10 years had passed since the completion of construction of tunnel. Therefore, the state of invert concrete lining was investigated by taking off the road bed material. As a result, it was found that shear failure had occurred at the junction between the invert and sidewall foot and an upheaval with a height of 170mm had occurred at the invert center. In addition, the top heading arch convergence of 376mm was obtained by measurement on the inner tunnel space, though no slippage at the construction junction between the top heading arch and sidewall was observed. Figure 4 shows the detail of failure occurred at the junction between the invert and sidewall foot. The ground at tunnel site and its vicinity, where the tunnel deformation occurred, appeared to

be composed of mudstone and tuff with the uniaxial compressive strength of  $8.4\text{N/mm}^2$  and  $11.6\text{N/mm}^2$ , respectively. The overburden height at the section where deformation occurred is 120m.

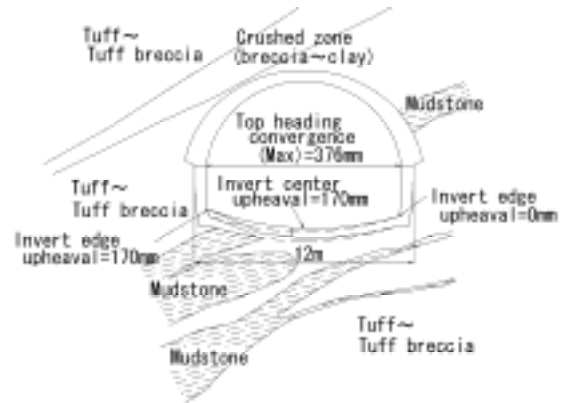


Figure 3. Deformation and geotechnical profile of Tunnel B.



Figure 4. Detail of failure occurred at junction between tunnel invert and sidewall foot in Tunnel B.

## 3 ESTIMATION OF FAILURE MECHANISM OF DAMAGED TUNNELS

### 3.1 Outline of the analysis

For the purpose of clarifying the mechanism of the failure of damaged tunnels and estimating the direction and magnitude of earth pressure acting on concrete lining, FEM analysis considering the occurrence and development of cracks was carried out. In this analysis, nonlinear finite element method was used and modified Newton-Raphson method was adopted for the solution of nonlinear equations. Plane-stress elements for material and Kupfer's failure criterion were adopted (Mashimo et al. 2004).

Figure 5 shows the stress-strain relation in compression and tension adopted in the analysis. The curve in compression was modified as quadric curve until strain reached the ultimate compressive strain -  $3,500 \times 10^{-6}$ . No stiffness decrease was defined after that. The curve in tension was regulated by tensile-softening curve. The tensile strength  $f_t$  was calculated on the basis of compressive strength  $f_c$  as  $f_t = 0.23f_c^{2/3}$ . Allowable crack width and ratio of resid-

ual strength  $\mu$  in concrete was set as 0.02mm and 1.0, respectively. The interaction between tunnel lining and ground was modeled by a series of spring support outside the tunnel lining, which were assumed to resist only compression and had zero stiffness when subjected to tension. The coefficient  $k$  of subgrade reaction was obtained from the following Eq.(1):

$$k=1/0.3\alpha E(B/0.3)^{-3/4} \quad (1)$$

where  $\alpha$  = correction factor(=0.4);  $E$  = Young's modulus of ground;  $B$  = tunnel height.

The mechanical properties of tunnel lining adopted in the FEM analysis are listed in Table 1.

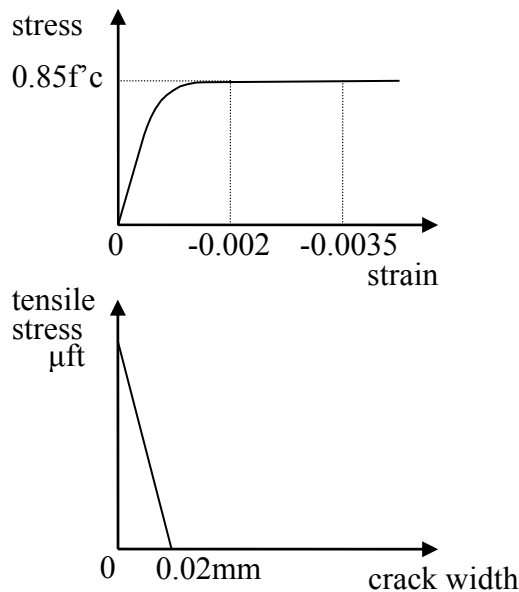


Figure 5. Stress-strain relation adopted in analysis.

Table 1. Mechanical properties adopted in analysis.

Item	
Design compressive strength : $\sigma'_{ck}$ [N/mm <sup>2</sup> ]	18
Compressive strength of concrete: $f'_c$ [N/mm <sup>2</sup> ]	18
Tensile strength of concrete: $f_t$ [N/mm <sup>2</sup> ]	1.579
Fracture energy of concrete: $G_f$ [N/m]	1.579
Poisson's ratio of concrete : $\nu$	0.2
Initial elastic modulus of concrete [kN/mm <sup>2</sup> ]	22
Modulus of subgrade spring [MN/m <sup>3</sup> ]	4.3 (TunnelA) 96 (TunnelB)

Figure 6 shows the outline of analysis model of Tunnel A. In the calculation of Tunnel A, for the purpose of estimating the direction and magnitude of earth pressure acting on the concrete lining, two kinds of load condition and the arrangement of subgrade springs were adopted. In model 1, earth pressure acted on the concrete lining throughout the whole top heading arch and sidewall in the horizontal direction and there was no subgrade spring outside the concrete lining because void was found behind the crown. In model 2, earth pressure acted on the concrete lining throughout the top heading arch partially in the direction at an angle of 45 or 75 de-

gree from the horizontal and the sidewall was supported by subgrade springs. In the calculation, attention was given to tensile cracks at the shoulders and the compressive failure at the crown due to bending moment to evaluate the validity of analysis on the deformation of concrete lining.

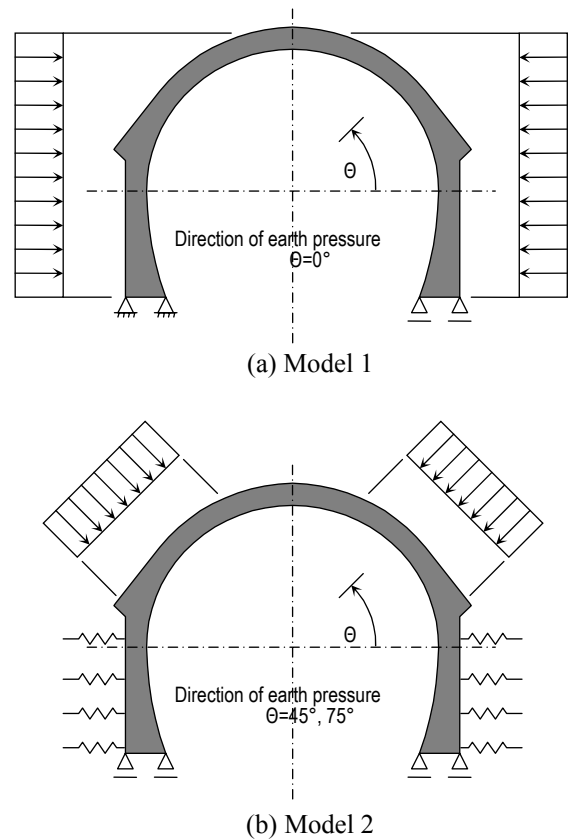


Figure 6. Outline of analysis model of Tunnel A.

Figure 7 shows the outline of analysis model of Tunnel B. In the calculation of Tunnel B, whole concrete lining with invert was supported by subgrade springs. Construction joint between the top heading arch and sidewall was modeled by interface elements, which consisted of spring element in the normal and tangential direction. Four kinds of load conditions were adopted to estimate the direction and magnitude of earth pressure acting on concrete lining. In model 1, earth pressure acted on the invert in the vertical direction. In model 2, earth pressure acted on the concrete lining throughout the top heading arch and sidewall in the horizontal direction. In model 3, earth pressure acted on the concrete lining throughout the top heading arch in both the vertical and horizontal direction, sidewall in the horizontal direction and invert in the vertical direction. In model 4, earth pressure acted on the concrete lining throughout the whole top heading arch in the horizontal direction and the sidewall foot partially in the horizontal direction. In this model, the magnitude of earth pressure acting on the sidewall was assumed to be far larger than that acting on the top heading arch. In the calculation of every model, attention was

given to the shear failure occurred at the joint between the invert and sidewall foot.

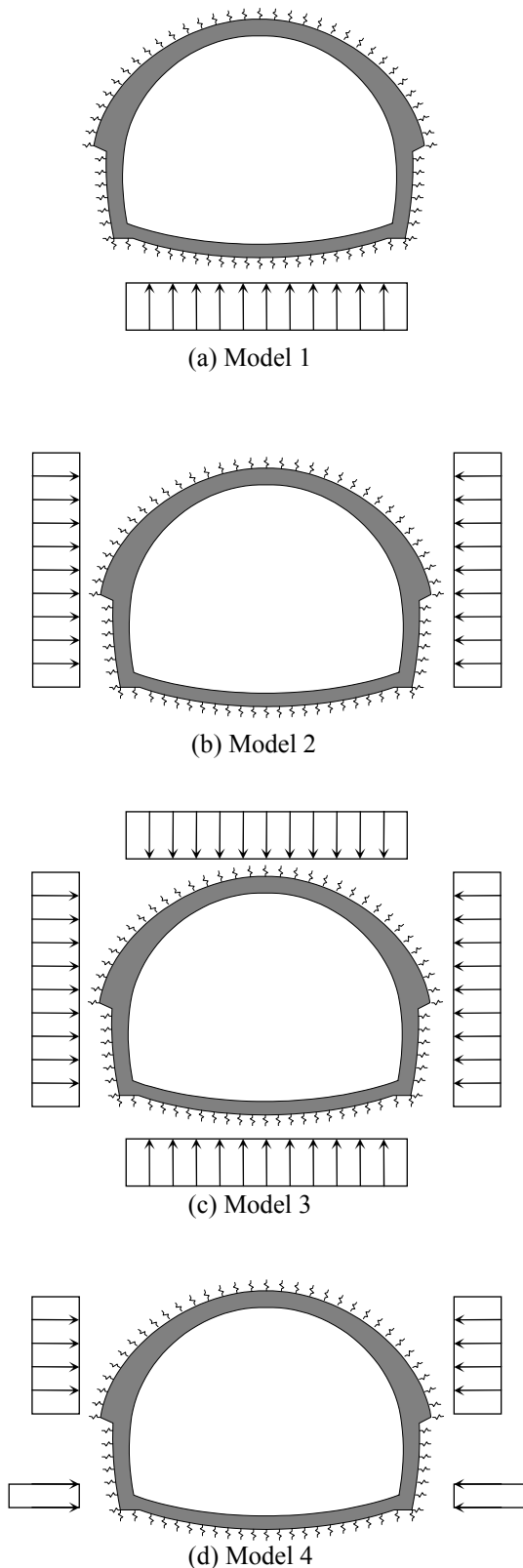


Figure 7. Outline of analysis model of Tunnel B.

### 3.2 Estimation of earth pressure acting on concrete lining

Figure 8 shows the state of the cracks obtained by numerical analysis on Tunnel A. It can be seen that

in the analysis model 1, tensile cracks occurred at the inside of the sidewall and at the outside of the crown. The compressive strains occurred at the inside of the crown showed a value above  $3,000\mu$  and it was assumed that compressive failure occurred at the crown. However, tensile cracks at the shoulders did not occur. On the other hand, in model 2, tensile cracks occurred at the inside of the shoulders and at the outside of the crown in both cases of  $\theta=45$  and  $75^\circ$ . The compressive strain occurred at the inside of the crown also showed a value greater than the ultimate compressive strain of  $-3,500 \times 10^{-6}$  and it was assumed that compressive failure occurred at the crown in both cases. Therefore, it can be assumed that model 2 is more suitable than model 1 for simulating the state of deformation occurred in tunnel A. This means that deformation of Tunnel A was not induced by earth pressure acting on the concrete lining in the horizontal direction, but in the slanting direction.

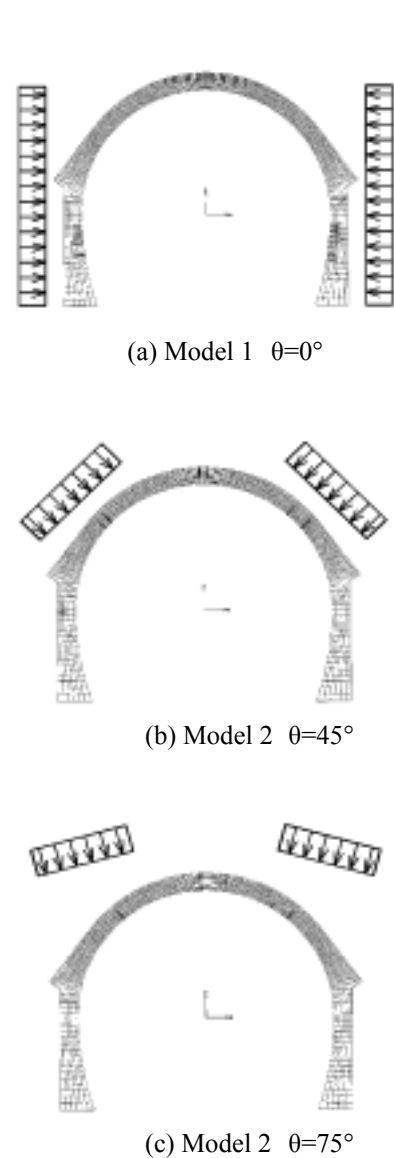


Figure 8. State of cracks obtained by analysis on Tunnel A.

Figure 9 shows the relationship between tunnel displacement at crown and earth pressure acting on

concrete lining obtained numerical analysis using model 2 on Tunnel A. Tensile cracks occurred at the inside of the shoulders when the earth pressure reached approximately 130kPa and 250kPa in the case of  $\theta=45^\circ$  and  $75^\circ$ , respectively, and shortly afterward tensile cracks occurred at the outside of the crown. When the earth pressure reached 515 kPa and 215kPa in the case of  $\theta=45^\circ$  and  $75^\circ$ , respectively, the strain of the inside of the crown exceeded the ultimate compressive strain and it was assumed that compressive failure occurred at these earth pressure values. The overburden height corresponding to these earth pressure values were calculated at approximately 9m and 20m by using the unit weight of ground mass  $\gamma=25\text{kN/m}^3$ . Overburden height of 9m in the case of  $\theta=45^\circ$  is almost the same height of loosened area estimated from the elastic wave velocity distribution of the ground.

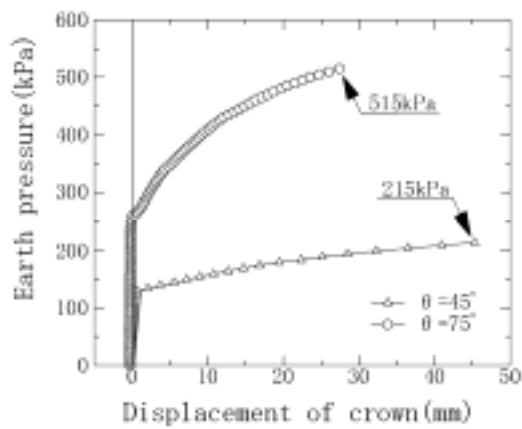
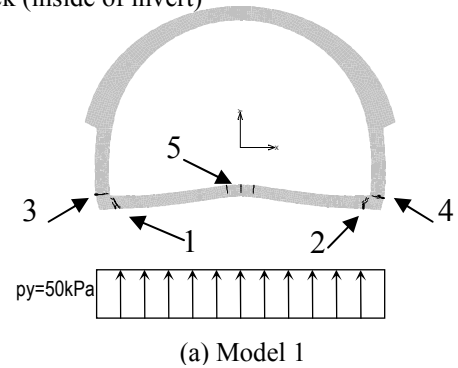


Figure 9. Earth pressure-displacement curve.

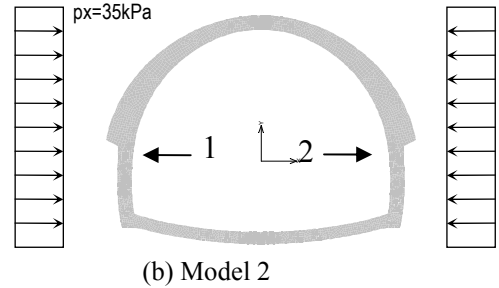
Figure 10 shows the state of the cracks obtained by numerical analysis on Tunnel B. In model 1, tensile cracks occurred at the inside of the invert center and at the outside of the invert edge and sidewall foot when the earth pressure acting on the invert reached 50kPa. In model 2, slippage at the construction joint between the top heading arch and sidewall occurred when the earth pressure acting on the concrete lining in the horizontal direction reached 35kPa, though no tensile crack occurred. In model 3, tensile cracks occurred at the outside of the invert edge and sidewall foot when the earth pressure acting on the concrete lining in both the horizontal and vertical direction reached 50kPa. In model 4, tensile cracks occurred at the outside of the sidewall and splitting cracks occurred at the invert edge, when the earth pressure acting on the top heading arch and sidewall foot in the horizontal direction reached 515kPa and 12,500kPa, respectively. Therefore we can conclude that shear failure occurred at the junction between the invert and sidewall was induced by excessive earth pressure acting on the tunnel sidewall foot in addition to that on the top heading arch in the horizontal direction. However, the earth pressure of 12,500kPa acting on the sidewall foot is far

larger than the overburden earth pressure of 3,000kPa obtained by using the unit weight of ground mass  $\gamma=25\text{kN/m}^3$ .

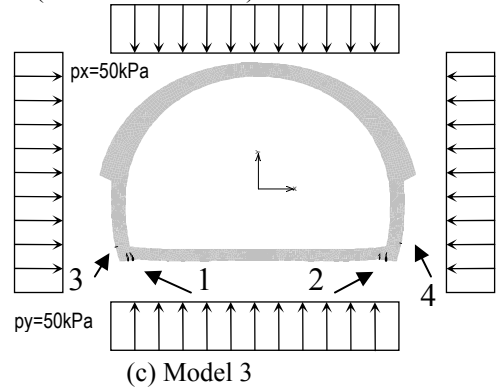
- 1,2:Crack (outside of invert )
- 3,4.Crack (outside of sidewall)
- 5 :Crack (inside of invert)



- 1,2:Slippage (construction joint) #no crack



- 1,2:Crack(outside of invert )
- 3,4. Crack(outside of sidewall)



- 1,2:Splitting crack (invert )
- 3,4. Crack (outside of sidewall)

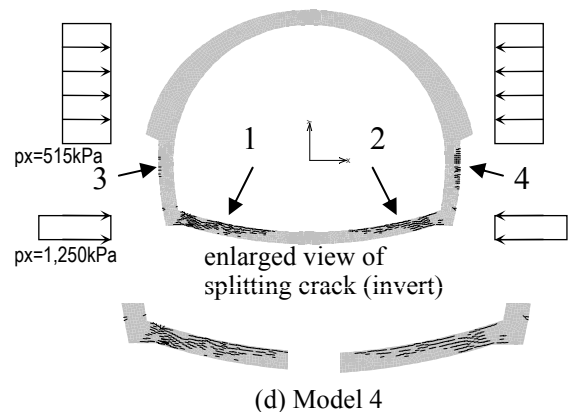


Figure 10. State of cracks obtained by analysis on Tunnel B.

## 4 CONCLUSION

In this study, field inspection on the damaged tunnels and numerical analysis using FEM were carried out to clarify the mechanism of the failure of concrete lining by the action of excessive earth pressure. The main conclusions obtained from the study are as follows.

1) Excessive earth pressure acting on tunnel lining could induce compressive failure at tunnel crown or shear failure at junction between sidewall and invert

2) FEM analysis considering the occurrence and development of cracks is effective in estimating the failure mechanism of damaged tunnel concrete lining by the action of excessive earth pressure.

## 5 REFERENCES

Mashimo,H.,Isago,N&Kitani,T. 2004. Numerical approach for design of tunnel concrete lining considering effect of fiber reinforcements , Tunnelling and Underground Space Technology , Vol.19 , No.4-5: 454-455.